THEORY OF ELASTIC DIFFERENTIAL SCATTERING IN LOW ENERGY HE^+ + HE COLLISIONS

Raymond P. Marchi and Felix T. Smith*

Stanford Research Institute

December 21, 1964

ABSTRACT

The elastic differential scattering of He^+ in He is calculated at the barycentric energies 15, 50, and 300 eV for comparison with the experiments of Lorents and Aberth (preceding paper). We use available computed potentials of the *g* and *u* states of He_2^+ dissociating smoothly to ground state He^+ + He. The quantal interference pattern is reproduced by applying the principle of superposition to the classical scattering amplitudes appropriate to the pure *g* and *u* states, *i.e.*, amplitudes whose magnitudes and phases are given by classical integrals over the trajectories corresponding to the *g* and *u* potentials separately. The interference takes place at the common angle θ, and usually involves different values of the angular momentum in the 2 states. Non-zero minima occur even in 2-state elastic scattering because the 2 interfering terms may differ in magnitude. A secondary interference at large angles is identified as an effect of nuclear symmetry that should disappear in an experiment using 2 different isotopes. It is likely that all the details seen in the elastic scattering experiments at these energies can be accounted for quantitatively by the 2-state theory, but to explain the data at the lowest energies and those at the largest angles would require knowledge not now available of the behavior of the potentials at large and small *R*.

I INTRODUCTION

The calculations we are reporting here of the scattering of He^+ by He were provoked by the fascinating experimental data of the preceding paper by Lorents and Aberth[1]. Just as their work is intimately related to the experiments of Everhart and his associates[2] on symmetric charge-exchange scattering, so the theory is related to an even longer history, beginning with the classic work of Mott[3] and of Massey and Smith[4]. Indeed, the basic theory we shall need is already present in those papers of more than thirty years ago. It is a mark of the natural forgetfulness of physicists, ameliorated only by the memory on our library shelves, that the remarkable oscillations first seen by Everhart were greeted by many of us a few years ago with startled surprise and even incredulity.

The special features of collisions between identical particles in quantum mechanics were first investigated by Mott in connection with the scattering of α particles by He nuclei. Massey and Smith[4] applied similar considerations to $He^+ - He$ scattering in their study of the motion of positive ions through gases, and derived the basic formulas we shall use. They ultimately calculated a total cross section, using potentials for He_2^+ due to Pauling[5], but they could have computed differential cross sections as well. Their expression for the differential scattering amplitude clearly displays itself as a sum of independent terms whose interference would create just the sort of oscillating pattern Everhart found.

Little theoretical work was done on atomic differential scattering cross sections between 1933 and 1959, but much was done on total cross sections. Among other developments, the impact parameter approximation became popular for collisions at moderately high energies—in this, the nuclei are considered to move classically and undeflected along their initial trajectory, and the electronic motion is treated in the slowly varying potential due to the moving nuclei. This picture was applied immediately to the interpretation of Everhart's data on the oscillating charge transfer probability as a function of collision velocity in the small-angle scattering of He^+ by He.[6]

I INTRODUCTION

The calculations we are reporting here of the scattering of He^+ by He were provoked by the fascinating experimental data of the preceding paper by Lorents and Aberth[1]. Just as their work is intimately related to the experiments of Everhart and his associates[2] on symmetric charge-exchange scattering, so the theory is related to an even longer history, beginning with the classic work of Mott[3] and of Massey and Smith[4]. Indeed, the basic theory we shall need is already present in those papers of more than thirty years ago. It is a mark of the natural forgetfulness of physicists, ameliorated only by the memory on our library shelves, that the remarkable oscillations first seen by Everhart were greeted by many of us a few years ago with startled surprise and even incredulity.

The special features of collisions between identical particles in quantum mechanics were first investigated by Mott in connection with the scattering of α particles by He nuclei. Massey and Smith[4] applied similar considerations to $He^+ - He$ scattering in their study of the motion of positive ions through gases, and derived the basic formulas we shall use. They ultimately calculated a total cross section, using potentials for He_2^+ due to Pauling[5], but they could have computed differential cross sections as well. Their expression for the differential scattering amplitude clearly displays itself as a sum of independent terms whose interference would create just the sort of oscillating pattern Everhart found.

Little theoretical work was done on atomic differential scattering cross sections between 1933 and 1959, but much was done on total cross sections. Among other developments, the impact parameter approximation became popular for collisions at moderately high energies—in this, the nuclei are considered to move classically and undeflected along their initial trajectory, and the electronic motion is treated in the slowly varying potential due to the moving nuclei. This picture was applied immediately to the interpretation of Everhart's data on the oscillating charge transfer probability as a function of collision velocity in the small-angle scattering of He^+ by He.[6]

In such a colliding system one of the electrons on the initially neutral He sees an equivalent unoccupied orbital (with the same spin) on the approaching He^+. In the symmetric potential due to the nuclei and the other 2 electrons, the mobile electron may be thought of as oscillating back and forth across the potential well while the two nuclei are close together, and tunnelling through the intervening barrier when they are somewhat further apart; the charge transfer probability depends on the phase of the oscillation in which the electron is left when the nuclei separate so far that further tunnelling is negligible. This physical picture corresponds to a time-dependent wave function that can conveniently be written as a linear combination of symmetric and antisymmetric wave functions for states of the molecular system He_2^+. As long as the nuclei are not moving too fast, it seems reasonable to hope that the motion can be described fairly well by using just the two states, one gerade and one ungerade, that dissociate smoothly to the ground state ion and atom. At the beginning of the collision, when the atom and ion are far apart, the relative phase of the g and u functions must be chosen so that the third electron is localized on the proper atom; the relative phase at the end of the collision determines the probability of finding the electron on the same atom. According to this model, the charge transfer probability oscillates between 0 and 1.

Everhart and his associates[2b] have measured the charge transfer probability of He^+ in He at energies from about 400 ev to 2×10^5 ev and angles from 0.3° to 5°. The oscillations they observe are in reasonable agreement with the theoretical calculations for the model just described, except for the fact that the charge transfer probability is "damped" so that its oscillations do not extend all the way to 0 or 1.

For such a 2-state theory, it is clear that the proper gerade potential to use at small R cannot be the lowest one,[6] but is the one that goes smoothly from the lowest dissociation limit of $He^+ + He$ to the $1s(2p)^2$ state of Be^+ in the united atom limit[7]. It is to be expected, in view of the Landau-Zener theory, that the curve crossings will be relatively ineffective in producing transitions to other states as long as the nuclear velocity is large in the neighborhood of the crossing point of the potential curves. However, the probability of such transitions is not zero, and these events are certainly responsible for some of the observed "damping" of the oscillations, as they are in the related case of $H^+ + H$ collisions.[8]

When Lorents and Aberth's ion scattering data began to appear, showing the same non-zero minima in the interference pattern, one of us began to examine the theory with the initial aim of looking at the excitation process as the cause of the damping. However, it soon became clear that even a 2-state theory, when properly formulated, would show such damping as a result of the interference of 2 scattering amplitudes that might have different magnitudes at the scattering angle.[9] This observation came essentially simultaneously with the experimental demonstration of apparent damping even at energies below the first excitation potential of He. Independently and at the same time, F. J. Smith[10] showed that the same effect is important in the $H^+ + H$ charge exchange at the lower end of the measured energy range. The effect is really not new, the relevant expressions being present in Massey and Smith's paper[4], and the same idea has been recognized in connection with spin-exchange scattering and elsewhere. In the energy range of interest here, the scattering amplitudes that interfere can be computed purely classically provided they are each given a classical phase (a standard action integral) as well as the usual magnitude.

We have therefore limited our attention for the present to the 2-state theory, which we apply here to calculations that can be compared with Lorents and Aberth's experiments. We have used existing potential energy curves, that of Reagan, Browne and Matsen[11] for the u curve and that of Phillipson[12] and Lichten[7] for the g curve. We first calculated the direct ion-atom scattering, ignoring the symmetry in the nuclei, and found very satisfactory agreement with the experiments at low and intermediate angles. When the nuclear symmetry was introduced in addition, an additional oscillation appeared in the large angle region that could immediately be identified with the subsidiary structure seen in this region of the experimental curves.

II GENERAL THEORY

A. SEPARATION OF ELECTRONIC AND NUCLEAR MOTION

If the nuclear motion is described by the relative coordinate vector $\mathbf{R}$, and the electrons by the coordinates $\mathbf{r}_i$ or simply $\mathbf{r} = (\mathbf{r}_1, \mathbf{r}_2, \mathbf{r}_3)$, we can write the total potential energy as the sum of an electronic part and a purely nuclear repulsion

$$U(\mathbf{R},\mathbf{r}) = U^{el}(R;\mathbf{r}) + \frac{4e^2}{R} \quad , \tag{1}$$

where the direction of $\mathbf{R}$ does not enter as long as the vectors $\mathbf{r}_i$ are measured in a relative coordinate system rotating with $\mathbf{R}$. The total wave function is expanded in terms of molecular electronic wave functions depending on $\mathbf{R}$ as a parameter[13]

$$\psi(\mathbf{R},\mathbf{r}) = \sum_j \psi_j^{nu}(\mathbf{R})\psi_j^{el}(\mathbf{R};\mathbf{r}) \quad . \tag{2}$$

Because of the complete symmetry of the potential (1) upon inversion in the center of mass, the functions ψ_j^{el} fall into two orthogonal families labelled g and u; we shall use only one of each, so j will take only two values, $j = (g,u)$. By integrating over the electronic coordinates, the electronic energy is defined for each of these states as a function of R:

$$E_{g,u}^{el}(R) = \int \psi_{g,u}^{el*}(R,\mathbf{r})[T^{el} + U^{el}(R;\mathbf{r})]\psi_{g,u}^{el}(R,\mathbf{r})d^9\mathbf{r} \quad . \tag{3}$$

As $R \to \infty$, E_g^{el} and E_u^{el} both approach E_∞^{el}, the (negative) sum of the binding energies of the electrons in the ground state atom and ion. By combining each $E^{el}(R)$ with the nuclear repulsive energy and E_∞^{el} we obtain the adiabatic potentials for the nuclear motion in the g and u states:

$$V_{g,u}(R) = E_{g,u}^{el}(R) - E_\infty^{el} + \frac{4e^2}{R} \quad . \tag{4}$$

In the limit as $R \to \infty$, the states ψ_g^{el} and ψ_u^{el} are linear combinations of the states ψ_A^{el}, representing the initial ion-atom pair, and ψ_B^{el},

representing the charge-transferred pair:

$$\psi_A(\mathbf{r}) = \lim \frac{1}{\sqrt{2}} (\psi_u + \psi_g) \quad , \tag{5a}$$

$$\psi_B(\mathbf{r}) = \lim \frac{1}{\sqrt{2}} (\psi_u - \psi_g) \quad ; \tag{5b}$$

at the beginning of the collision ψ_u and ψ_g are in phase as in (5a), but there is no reason for them to be so at the end since the g and u phases develop differently during the collision.

B. CLASSICAL NUCLEAR MOTION

Later in this paper we shall discuss the quantal nuclear motion in the framework of time-independent scattering theory, but here we follow the earlier treatments of the $He^+ - He$ problem[6,7] in assuming classical nuclear motion and looking at the time-dependent theory of the electronic motion. The time-dependent electronic wave functions can then be written approximately in the form

$$\psi_j^{el}(R;\mathbf{r},t) = \psi_j^{el}(R;\mathbf{r}) e^{i\gamma_j(t)} \quad , \qquad (j = g,u) \tag{6}$$

where, since R is varying slowly,

$$\gamma_j(t + \delta t) = \gamma_j(t) + E_j^{el}(R) \frac{\delta t}{\hbar} \quad . \tag{7}$$

It is convenient to factor out the phase factor, common to the g and u functions, describing the evolution of the system when R is large,

$$e^{iE_\infty^{el} t/\hbar} \quad .$$

The wave functions after the collision is over then become

$$\psi_j^{el}(R;\mathbf{r},t) \rightarrow \psi_j^{el}(R;\mathbf{r}) e^{iE_\infty^{el} t/\hbar} e^{i\eta_j} \quad , \tag{8}$$

where

$$\eta_j = \hbar^{-1} \int_{-\infty}^{\infty} \{E_j^{el}[R(t)] - E_\infty^{el}\} dt$$

$$= 2\hbar^{-1} \int_{r_0}^{\infty} [E_j^{el}(R) - E_\infty^{el}] \dot{R}^{-1} dR \quad . \tag{9}$$

The final phase difference between the g and u functions is then

$$\eta_u - \eta_g \ . \tag{10}$$

The initial wave function $\psi_A(\mathbf{r})$ evolves into

$$\frac{1}{\sqrt{2}} (\psi_u e^{i\eta_u} + \psi_g e^{i\eta_g}) = \frac{1}{2} \psi_A (e^{i\eta_u} + e^{i\eta_g}) + \frac{1}{2} \psi_B (e^{i\eta_u} - e^{i\eta_g}) \quad . \tag{11}$$

The probabilities of elastic scattering P_{AA} and of charge transfer P_{AB} are then

$$P_{AA} = \frac{1}{2} [1 + \cos(\eta_u - \eta_g)] \quad , \quad P_{AB} = \frac{1}{2} [1 - \cos(\eta_u - \eta_g)] \quad . \tag{12}$$

The phases η_i are functions both of the relative kinetic energy

$$E = \frac{\mu}{2} \dot{R}_\infty^2 = \frac{\mu}{2} v_\infty^2 \tag{13}$$

and of the relative angular momentum L or impact parameter b,

$$L^2 = 2\mu E b^2 \quad . \tag{14}$$

Since the scattering angle θ is determined by L and E, the phases can also be taken as functions of E and θ, $\eta_i(E,\theta)$. To compute these functions by (9) one needs the functional form $R(t)$ or its equivalent, the radial velocity

$$\dot{R}(R) = v(R) = v(E,L;R) \ , \tag{15}$$

and also the turning point

$$r_0 = r_0(E,L) \tag{16}$$

for the lower limit of integration. These quantities v and r_0 can be chosen with various degrees of refinement:

Case (i)

$$v^{(i)}(R) = v_\infty = \left(\frac{2E}{\mu}\right)^{1/2} , \tag{16a}$$

$$r_0^{(i)} = 0 . \tag{16b}$$

This approximation seems justified at high enough energies and large enough angles (small enough L), where the electronic energies $E_j^{el}(R)$ near the turning point r_0 are already close to the united-atom value $E_j^{el}(0)$. This assumption is confirmed by the observation[2b] of a region ($E \cdot \theta \gtrsim 2 \times 10^4$ deg-ev) where the charge transfer probability depends only on E and not on θ.

Case (ii)

$$v^{(ii)}(R) = v_\infty\left(\frac{1 - b^2}{R^2}\right)^{1/2} , \tag{17a}$$

$$r_0^{(ii)} = b . \tag{17b}$$

This is the standard impact-parameter approximation, and is valid at energies and angles somewhat smaller than (i).

Case (iii)

$$v^{(iii)}(R) = v_\infty\left[1 - \left(\frac{b^2}{R^2}\right) - \frac{V_{av}(R)}{E}\right]^{1/2} , \tag{18a}$$

$$[r_0^{(iii)}]^2\{1 + V_{av}[r_0^{(iii)}]\} = b^2 \tag{18b}$$

where

$$V_{av}(R) = \frac{1}{2}[V_u(R) + V_g(R)] . \tag{18c}$$

This assumes that the classical nuclear motion occurs under the influence of the average potential (18c), and has been frequently employed. Its range of validity extends to still smaller energies and angles than (i) and (ii); we shall show later that the particular average (18c) is justified by the more exact theory. Closely related to case (iii) is one of the approximations used by Bates and Boyd[14], in which V_{av} is replaced by a pure coulomb potential V_C.

Case (iv)

$$v_j(R) = v_\infty \left[1 - \left(\frac{b^2}{R^2} \right) - \frac{V_j(R)}{E} \right]^{1/2} , \qquad (19a)$$

$$[r_{0j}^{(iv)}]^2 \{ 1 + V_j [r_{0j}^{(iv)}] \} = b^2 . \qquad (19b)$$

Here we take note of the fact that the nuclear trajectories may be different in the g and u states, so that different velocities and turning points must be used in the integrals (9) for η_u and η_g. The phase difference $\eta_u - \eta_g$ obtained in this way was used by Bates and Boyd[14] as the basis for an expansion which they applied to the calculation of total cross sections. As we shall see, the final result for the theory of differential cross sections is somewhat different, but (19) emphasizes the essential point that at low energies the nuclear trajectories in the 2 states are different.

The phases η_u and η_g obtained from (9) by using (16) through (19) are expressed in terms of E and L, not directly as functions of E and θ. A relation between θ and L follows from the classical dynamics of the collision provided a non-zero potential $V(r)$ governs the nuclear motion. This relation has usually been obtained by using the assumptions of Case (iii). When the angle involved is not too large, Everhart[2c] has made use of a high energy approximation in which the product $E\theta$ has especially simple properties—this can be shown[15] to represent the first term in the expansion of $\theta(E,L)$ in powers of E^{-1}. If Case (iv) is followed, one finds two different scattering angles $\theta_j(L)$ associated with a single value of L, or two different angular momenta $L_j(\theta)$ associated with the same angle. That this conclusion is correct will be shown when we consider the quantal nature of the nuclear motion

C. QUANTAL AND SEMICLASSICAL NUCLEAR MOTION

1. Without Nuclear Symmetry

Instead of assuming classical nuclear motion, we return to the quantal representation of Eq. (2) and consider the nuclear part of the scattering represented by the functions $\psi_j^{nu}(\mathbf{R})$. After the Born-Oppenheimer separation of coordinates, these functions each satisfy a nuclear Schrödinger equation with the appropriate potential $V_j(R)$ from Eq. (4). The radial symmetry permits the usual partial wave separation of the $\psi_j^{nu}(\mathbf{R})$. The complete wave function for the scattered wave after the collision then has the form

$$\begin{aligned}\psi &\to 2^{-\frac{1}{2}}R^{-1}e^{ikR}\{f_u(\theta,E)\psi_u^{el}(\mathbf{R},\mathbf{r}) + f_g(\theta,E)\psi_g^{el}(\mathbf{R},\mathbf{r})\} \\ &= (2R)^{-1}e^{ikR}\{(f_u + f_g)\psi_A^{el} + (f_g - f_u)\psi_B^{el}\} \quad . \end{aligned} \tag{20}$$

The differential cross sections for direct scattering, σ_{AA}, and for charge exchange scattering, σ_{AB}, are then[4]

$$\begin{aligned}\sigma_{AA}(E,\theta) &= \frac{1}{4}\left|f_u(E,\theta) + f_g(E,\theta)\right|^2 \quad , \\ \sigma_{AB}(E,\theta) &= \frac{1}{4}\left|f_u(E,\theta) - f_g(E,\theta)\right|^2 \quad , \end{aligned} \tag{21}$$

and the corresponding probabilities are

$$\begin{aligned}P_{AA}(E,\theta) &= \frac{\sigma_{AA}}{\sigma_{AA} + \sigma_{AB}} \quad , \\ P_{AB}(E,\theta) &= \frac{\sigma_{AB}}{\sigma_{AA} + \sigma_{AB}} \quad . \end{aligned} \tag{22}$$

These probabilities can attain the limits 1 and 0 only if $|f_u| = |f_g|$.

In Eqs. (20) and (21) the entire phase factor (both nuclear and electronic) is embodied in the scattering amplitudes $f_j(\theta,E)$, which are constructed in the usual way:

$$f_j(\theta,E) = \frac{1}{2ik}\sum_l (2l+1)(e^{2i\delta_l^j(E)} - 1)P_l(\cos\theta) \quad , \quad (j = g,u) \quad . \tag{23}$$

The phases $\delta_l^g(E)$ and $\delta_l^u(E)$ can be found from the asymptotic behavior of the appropriate nuclear radial wave functions. For accurate evaluation, these functions should be obtained by solving the radial wave equations with the potentials $V_g(R)$, $V_u(R)$. At the energies of interest here, however, a semiclassical treatment is appropriate[16,17], and the classical phases $\Delta_g(L,E)$, $\Delta_u(L,E)$ can be used along with the correspondence relations:

$$\left(l + \frac{1}{2}\right)\hbar \longrightarrow L \quad , \quad 2\hbar\delta_l(E) \longrightarrow \Delta(L,E) \quad . \tag{24}$$

The classical phase[15] is an action integral over the effective classical *radial* motion:

$$\Delta_j(L,E) = 2\int_{r_{0j}}^{\infty}\left\{2\mu[E - V_j(r)] - \frac{L^2}{r^2}\right\}^{1/2} dr - 2\int_b^{\infty}\left[2\mu E - \frac{L^2}{r^2}\right]^{1/2} dr \tag{25}$$

$$= \int_{r_{0j}}^{\infty}\left\{2\mu\left[E - V_j(r)\right] - \frac{L^2}{r^2}\right\}^{1/2}[E - V_j(r)]^{-1}r\,\frac{dV_j}{dr}\,dr \quad . \tag{25a}$$

The scattering amplitudes f_j can be evaluated by direct numerical summation of the partial wave series (23) using the correspondence (24) and the classical approximation (25) for the phases; this common procedure has no simple appellation, and we recommend calling it the *semiquantal* summation, because the l's are taken quantally even though classical phases are used. Proceeding a step further, the usual semiclassical arguments allow us to approximate $f_j(\theta)$ by its classical limit which can be derived entirely from the classical phase function $\Delta_j(L,E)$:

$$f_j^{cl}(E,\theta) = [\sigma_j^{cl}(E,\theta)]^{1/2}e^{i\gamma_j(E,\theta)} \quad , \tag{26}$$

$$\sin\theta\ \sigma_j^{cl}(E,\theta) = \frac{\pi}{\mu E}\left(L\left|\frac{\partial^2\Delta_j}{\partial L^2}\right|^{-1}\right)_{L=L_j(E,\theta)} \quad , \tag{26a}$$

$$\hbar\gamma_j(E,\theta) = A_j(E,\theta) = \left[\Delta_j(E,L) - \theta L\left(\frac{\Theta_j}{|\Theta_j|}\right)\right]_{L=L_j(E,\theta)} + \hbar\alpha_j \quad , \tag{26b}$$

$$\alpha_j = \frac{5\pi}{4} + \frac{\pi}{2}\left(\frac{\Theta_j}{|\Theta_j|}\right) + \frac{\pi}{4}\left(\frac{\Delta_j''}{|\Delta_j''|}\right) \quad , \tag{26c}$$

$$\Theta_j(E,L) = \frac{\partial\Delta_j}{\partial L} = \Delta_j' \quad , \quad \theta = |\Theta| \quad , \tag{26d}$$

$$L_j(E,\theta) = L_j(E,|\Theta_j|) \quad , \tag{26e}$$

where (26e) represents the inverse of (26d).

In the energy range of interest, above 15 eV, the classical scattering amplitudes f_j^{cl} are very satisfactory approximations to the true f_j's. When these classical scattering amplitudes are combined we get the resultant amplitudes for direct and charge exchange scattering,

$$f_{AA} = \frac{1}{2}(f_u + f_g) \quad , \quad f_{AB} = \frac{1}{2}(f_g - f_u) \quad , \tag{27}$$

in the semiclassical approximation. The first nonclassical result to appear is an interference between two scattering amplitudes that may each validly be computed strictly classically. It is striking and significant that the *classical* scattering amplitudes, combined in the simplest way using the principle of superposition, suffice to give an excellent representation of the quantal results.

The success of the classical amplitudes $f_j^{cl}(\theta)$ suggests a physical picture. If two particles are thought of as colliding with a definite impact parameter b or angular momentum L. The incoming wave packet can be analyzed into two *coherent* parts, one in the gerade and the other in the ungerade electronic state. Each of them follows essentially the classical trajectory corresponding to its potential V_g or V_u, and is ultimately scattered predominantly through its own classical angle $\theta_g(L)$ or $\theta_u(L)$. If the observation is made at the angle $\theta = \theta_u(L)$, the gerade part of the packet will not be observed, since it is scattered mainly to some other angle. However, there is some different angular momentum, $L' = L_g(\theta)$, such that $\theta_g(L') = \theta = \theta_u(L)$, and the true scattering observed at the

angle θ is the interference between two coherent parts of a plane wave, the g part with angular momentum L and the u part with angular momentum L'. We must, in fact, relinquish a localized wave-packet picture of the scattering because we do not actually observe the impact parameter. Instead, we know the direction of motion of the initial and of the observed scattered beam, and therefore the angle of scattering θ. If we could measure the impact parameter, we would know less about the directional character of the motion, and the observations would be different. Indeed, the coherent interference between two widely separated regions of L is very similar to the interference between two parts of an optical wave front (or an electron beam) passing through a spatially separated pair of slits.

It is striking that the purely wave picture of the scattering which we are obliged to use is entirely compatible with a strictly classical approximation for the two scattering amplitudes that are interfering. In fact, a classical *quantity* (such as an action integral) may be an excellent approximation to the corresponding quantal one (such as the phase of a wave function or of a scattering amplitude) even when a classical *model* (such as a point particle trajectory) must be relinquished in favor of a complementary nonclassical one (such as a wave picture).

One reason for the "damping" in the charge transfer probability is now clear. The two amplitudes $f_u(E,\theta)$ and $f_g(E,\theta)$ will generally be different in magnitude, because of differences in both of the factors in $\sigma_j(E,\theta)$: $L_g(\theta) \neq L_u(\theta)$ and $\partial L_g/\partial\theta \neq \partial L_u/\partial\theta$ (except by accident at isolated points).

The cross sections of Eq. (21) will include an oscillating part containing the factor

$$\cos\,[\gamma_u(E,\theta) - \gamma_g(E,\theta)] \quad . \tag{28}$$

It is not hard to see that the phase difference $\eta_u - \eta_g$ of Eq. (12) as computed using the formulas (16) to (19) represents a set of varying approximations to the correct phase difference $\gamma_u - \gamma_g$. Since the latter is not hard to compute directly, the previous approximations will not be used in this work. However, the relation between the exact expression and the approximations will be given in the next section.

A note on terminology is in order: we advocate using the term "classical scattering amplitude" for the quantity calculated as in Eqs. (26) from a classical phase $\Delta(E,L)$. The term "semiclassical" can

be applied to any nonclassical amplitude that is computed from the classical phase by replacing the sum over l by an integral over L and using a modification of the method of stationary phase. This would include as "semiclassical" the rainbow and glory approximations of Ford and Wheeler,[17] and the interference of two or more classical amplitudes such as f_g and f_u. Finally, a "semiquantal amplitude" is one evaluated by using the exact partial wave summation over l, but using classical or semiclassical phases to approximate the quantal δ_l.

2. Connection Between Semiclassical and Classical Treatments

The connection between the semiclassical 2-state treatment and the classical results of Eqs. (16) to (19) will be established if we find out how the scattering parameters (especially the phases) change under a variation in the potential. In order to look into this, it is convenient to express the quantities of Eqs. (25) and (26) with the help of a reduced distance ρ related to the turning point R and of a reduced potential U:

$$\rho = r/R, \qquad U(R\rho) = V(r)/E \quad . \tag{29}$$

The angular momentum L is related to R by

$$L^2 = 2\mu E R^2 [1 - U(R)] \quad . \tag{30}$$

The functions whose variations we are interested in can be written as

$$(2\mu E)^{-\frac{1}{2}}\Delta = \pi R[1 - U(R)]^{\frac{1}{2}} - 2R + 2R \int_1^\infty (\rho^{-1}\{[1 - U(R\rho)]\rho^2 - [1 - U(R)]\}^{\frac{1}{2}} - 1)d\rho \ , \tag{31}$$

$$\Theta = \frac{\partial \Delta}{\partial L} = \pi - 2[1 - U(R)]^{\frac{1}{2}} \int_1^\infty \rho^{-1}\{[1 - U(R\rho)]\rho^2 - [1 - U(R)]\}^{-\frac{1}{2}}d\rho, \tag{31a}$$

$$A = \Delta - L\Theta + \hbar\alpha \tag{31b}$$

(where $\hbar\alpha$ is a constant), and

$$(\mu E/2)^{1/2}\Gamma = (\mu E/2)^{1/2}\frac{\partial^2\Delta}{\partial L^2}$$

$$= \{2[1-U(R)] - RU'(R)\}^{-1}\int_1^\infty \frac{\{U'(R)[1-U(R\rho)] - \rho U'(R\rho)[1-U(R)]\}d\rho}{\{[1-U(R\rho)]\rho^2 - [1-U(R)]\}^{3/2}} \qquad (31c)$$

These are all functionals of the potential and functions of R — and, by Eq. (30), so is L.

Consider any functional $F(U;R)$ depending on the parameter R and the function $U(R\rho)$. Under arbitrary small variations of R with the potential U unvaried the variation of F is $(\delta F)_U = (\partial F/\partial R)_U \partial R$, while the variation of F under a small change $\partial U(R\rho)$ in U but with fixed R can be written $(\delta F)_R$. The total variation in F is then, to first order,

$$DF = (\delta F)_R + (\partial F/\partial R)_U \delta R \quad . \qquad (32)$$

This relation can be applied to all of the functionals L, Δ, Θ, Γ, and A. When applied to A and Δ, some simplification arises from the identity

$$\left(\frac{\partial\Delta}{\partial R}\right)_U = \Theta\left(\frac{\partial L}{\partial R}\right)_U \qquad (33)$$

so that

$$DA + LD\Theta = D\Delta - \Theta DL = (\delta\Delta)_R - \Theta(\delta L)_R \quad . \qquad (34)$$

Thus the variation of A at fixed Θ is identical with the variation of Δ at fixed L; evaluating the right hand side of (34) by varying U in (30) and (31) we find

$$(\delta A)_\Theta = (\delta\Delta)_L = -(2\mu E)^{1/2}R\int_1^\infty \frac{\rho\delta U(R\rho)d\rho}{\{[1-U(r\rho)]\rho^2 - [1-U(R)]\}^{1/2}} \quad . \qquad (35)$$

We can now specialize the potentials, writing

$$U = \frac{1}{2}(U_g + U_u), \qquad \delta U_g = \frac{1}{2}(U_g - U_u) = -\delta U_u \quad . \qquad (36)$$

U is then the average potential, and $2\delta U_g$ is the difference potential. To first order in the potential difference, then

$$(\Delta_g - \Delta_u)_L = (A_g - A_u)_\Theta = -(2\mu E)^{1/2} R \int_1^\infty \frac{\rho[U_g(R\rho) - U_u(R\rho)]\,d\rho}{\{[1 - U(R\rho)]\rho^2 - [1 - U(R)]\}^{1/2}} \quad . \tag{37}$$

This is exactly the result of the classical approximation employing the average potential to describe the nuclear motion, Eqs. (18). That result is thus correct to first order in the potential difference. The remaining error in the phase difference is second order in the dimensionless function $[V_g(r) - V_u(r)]/E$, which usually attains its maximum value at $r = 0$. In the case of $He^+ + He$, this suggests that phase differences computed by Eq. (37) should become reliable at energies above about 1 kev. At lower energies we may expect deviations from Eq. (37), including deviations from its left hand equality which is only true to first order. In the low energy limit, then, the phase difference of Δ's at fixed L, which enters into the total cross section,[14] may differ from the phase difference of A's at fixed θ, which controls the interference pattern in the differential cross section.

Another important quantity that could be examined as an expansion in δU is the classical cross section σ. The leading term is of zero order in δU and determines the general trend, the upper envelope of the cross section curve. The non-zero lower envelope (the "damping" of the oscillations) appears first with the first order variation, that is, the term

$$(\delta\sigma)_\Theta = \pi(2\mu E \sin\theta)^{-1}\,\delta(L/\Gamma)_\Theta \quad . \tag{38}$$

We have not evaluated this, as it seemed better to compute σ_g and σ_u directly. However, it is interesting to see how $\delta\sigma$ enters into the upper and lower envelopes σ_+ and σ_-:

$$\sigma_+ = \left|\frac{1}{2}(\sigma + \delta\sigma)^{1/2} + \frac{1}{2}(\sigma - \delta\sigma)^{1/2}\right|^2 = \sigma - \delta\sigma^2/4\sigma \ldots, \quad (38a)$$

$$\sigma_- = \left|\frac{1}{2}(\sigma + \delta\sigma)^{1/2} - \frac{1}{2}(\sigma - \delta\sigma)^{1/2}\right|^2 = \delta\sigma^2/4\sigma \ldots \quad . \quad (38b)$$

3. Nuclear Symmetry

The expressions just given are appropriate for ion-atom scattering in which the electrons find themselves in a symmetric potential but where nuclear symmetry is ignored. The theory in that form is applicable to scattering of different isotopes of the same element. When identical atoms are involved an additional symmetry enters the problem. Because of the indistinguishability of the atoms, it is impossible to distinguish between direct scattering at θ and charge exchange scattering at $\pi - \theta$; since these events are coherent, there is interference between them. This interference appears in the wave function or the scattering amplitude. When the nuclei are bosons the total wave function must be even under a nuclear interchange, when they are fermions it must be odd. For ^{4}He, this means that the gerade electronic state is associated with a nuclear function that is symmetric on reflection about $\pi/2$, and the ungerade state has an antisymmetric nuclear wave function. The symmetrization is then accomplished by the substitutions[4]

$$f_g(\theta) \rightarrow f_g(\theta) + f_g(\pi - \theta) \quad ,$$

$$f_u(\theta) \rightarrow f_u(\theta) - f_u(\pi - \theta) \quad . \quad (39)$$

In place of Eq. (27), the scattering amplitudes for observing the ion, f_{AA}, and the neutral, f_{AB}, are:

$$f_{AA} = \frac{1}{2}[f_u(\theta) + f_g(\theta) - f_u(\pi - \theta) + f_g(\pi - \theta)] \quad , \quad (40)$$

$$f_{AB} = \frac{1}{2}[f_g(\theta) - f_u(\theta) + f_u(\pi - \theta) + f_g(\pi - \theta)] \quad . \quad (40a)$$

A simple alternative derivation can be given of the same result. Consider a plane wave ψ_A representing the collimated approach of A^+ to A,

where the nuclei are bosons. If ψ_A is analyzed in partial waves and the nuclear symmetry is considered, all the partial waves with l even must be associated with the g electronic state, and the l-odd waves with the u state.[16] The scattering amplitude is then

$$f_{AA}(E,\theta) = F_u(E,\theta) + F_g(E,\theta) \quad , \tag{41}$$

where

$$F_u(E,\theta) = \frac{1}{2ik} \sum_{l \text{ odd}} (2l+1)(e^{2i\delta_l^u} - 1)P_l(\cos\theta) \quad ,$$

$$F_g(E,\theta) = \frac{1}{2ik} \sum_{l \text{ even}} (2l+1)(e^{2i\delta_l^g} - 1)P_l(\cos\theta) \quad . \tag{42}$$

To reduce these to the classical approximation we must convert the sum to an integral, allowing l to take continuous values. However, we must preserve symmetry in doing so, which we can do by using the identity

$$P_l(\cos\theta) = (-)^l P_l[\cos(\pi-\theta)] = \frac{1}{2}\{P_l(\cos\theta) + (-)^l P_l[\cos(\pi-\theta)]\}. \tag{43}$$

We then can write

$$\begin{aligned} F_u(E,\theta) &= \sum_{l \text{ odd}} h_u(l,\theta) \\ &= \frac{1}{2} \sum_{\text{all } l} [h_u(l,\theta) - h_u(l,\pi-\theta)] \\ &\simeq \frac{1}{2}\left[\int_0^\infty h_u(l,\theta)dl - \int_0^\infty h_u(l,\pi-\theta)dl\right] \\ &\simeq \frac{1}{2}[f_u^{cl}(\theta) - f_u^{cl}(\pi-\theta)] \quad , \end{aligned} \tag{44}$$

and similarly

$$F_g(E,\theta) \simeq \frac{1}{2}\left[f_g^{cl}(\theta) + f_g^{cl}(\pi - \theta)\right] \quad . \tag{44a}$$

Substituting in (41) we get just the result of (40).

Let us write the classical scattering amplitudes in (40) in the form

$$\begin{aligned} B_1(E,\theta)e^{i\beta_1(E,\theta)} &= \frac{1}{2} f_u(E,\theta) \quad , \\ B_2(E,\theta)e^{i\beta_2(E,\theta)} &= \frac{1}{2} f_g(E,\theta) \quad , \\ B_3(E,\theta)e^{i\beta_3(E,\theta)} &= -\frac{1}{2} f_u(\pi - \theta) \quad , \\ B_4(E,\theta)e^{i\beta_4(E,\theta)} &= \frac{1}{2} f_g(\pi - \theta) \quad . \end{aligned} \tag{45}$$

The oscillating part of the cross section depends on the six difference frequencies $\beta_i - \beta_j$, of which 3 are independent; let us take these to be

$$\begin{aligned} \epsilon_{12}(E,\theta) &= \frac{1}{2}(\beta_1 - \beta_2) \quad , \\ \epsilon_{34}(E,\theta) &= \frac{1}{2}(\beta_3 - \beta_4) \quad , \\ \eta_{1234}(E,\theta) &= \frac{1}{2}(\beta_1 + \beta_2 - \beta_3 - \beta_4) = \epsilon_{13} + \epsilon_{24} \quad . \end{aligned} \tag{46}$$

With these, it is natural to express the complete cross section at small angles θ as a sum of a direct scattering cross section $\sigma_d(E,\theta)$, an exchange cross section $\sigma_e(E,\theta)$, and an interference term $S_{de}(E,\theta)$:

$$\sigma_{AA} = \sigma_d(E,\theta) + \sigma_e(E,\theta) + S_{de}(E,\theta) \quad , \tag{47}$$

$$\begin{aligned} \sigma_d(E,\theta) &= B_1^2 + B_2^2 + 2B_1B_2 \cos 2\epsilon_{12} \quad , \\ \sigma_e(E,\theta) &= B_3^2 + B_4^2 + 2B_3B_4 \cos 2\epsilon_{34} \quad , \end{aligned} \tag{48}$$

$$S_{de} = (B_1 + B_2)(B_3 + B_4) \cos \epsilon_{12} \cos \epsilon_{34} \cos \eta_{1234}$$
$$+ (B_1 + B_2)(B_3 - B_4) \cos \epsilon_{12} \sin \epsilon_{34} \sin \eta_{1234}$$
$$- (B_1 - B_2)(B_3 + B_4) \sin \epsilon_{12} \cos \epsilon_{34} \sin \eta_{1234}$$
$$+ (B_1 - B_2)(B_3 - B_4) \sin \epsilon_{12} \sin \epsilon_{34} \cos \eta_{1234} \quad . \quad (49)$$

At small and moderate angles θ we may expect the exchange cross section σ_e to be negligible by comparison with the direct cross section σ_d, and the interference term S_{de} to be intermediate in magnitude. Furthermore, we may hope to find the magnitudes of the B's such that S_{de} is dominated by its first term.

When θ is close to $\pi/2$, the symmetry relations (45) suggest combining the terms in σ_{AA} in a different way, writing

$$\sigma_u = \frac{1}{4} \left| f_u(E,\theta) - f_u(E, \pi - \theta) \right|^2 \quad ,$$
$$\sigma_g = \frac{1}{4} \left| f_g(E,\theta) + f_g(E, \pi - \theta) \right|^2 \quad , \quad (50)$$

together with an interference term $S_{ug}(E,\theta)$. The oscillations are then best described in terms of the phases ϵ_{13}, ϵ_{24} and $\eta_{1324} = \epsilon_{12} + \epsilon_{34}$, and an equation such as (49) can be rewritten to give S_{ug} by permuting the indices in the manner (1234) $\rightarrow$ (1324). Close to $\pi/2$, σ_g dominates and $\sigma_u \rightarrow 0$.

A feature of the experimental data that is readily examined is the movement of the interference maxima and minima with energy and angle. To predict this movement, let us consider combinations of the phases Δ_i in a general form, using A_i as defined in Eq. (26b),

$$\phi = \Sigma_i a_i A_i [E, L_i(\theta)] \quad , \quad (51)$$

of which Eq. (46) gives some specific examples. We may then examine the loci of constant ϕ in the (E,θ) plane. The slopes of these loci are given by $(\partial E/\partial\theta)_\phi$, to get which we use

$$\left(\frac{\partial \phi}{\partial E}\right)_{\theta} = \Sigma_i a_i \left(\frac{\partial \Delta_i}{\partial E}\right)_{L_i(\theta)} , \tag{52}$$

$$\left(\frac{\partial \phi}{\partial \theta}\right)_{E} = -\Sigma_i a_i b_i L_i(\theta) \tag{52a}$$

and

$$\left(\frac{\partial E}{\partial \theta}\right)_{\phi} = -\left(\frac{\partial \phi}{\partial \theta}\right)_{E} \Big/ \left(\frac{\partial \phi}{\partial E}\right)_{\theta} , \tag{52b}$$

where b_i is defined by

$$b_i \theta = \left(\frac{\partial \Delta_i}{\partial L}\right) , \quad b_i = \pm 1 . \tag{52c}$$

When $\phi = \epsilon_{12}$ or η_{1234}, a knowledge of the loci of constant ϕ combined with Eqs. (47) to (49) will provide information on the movement of the maxima and minima in question.

D. COUPLING OF STATES

We have employed an exclusively 2-state formulation in these calculations, and furthermore we have assumed that the symmetry of the potential excludes any mixing of the *g* and *u* states. The symmetry of the potential does indeed provide a very strong separation of *g* and *u* states, as long as the nuclei are identical; when the nuclei differ in mass, some coupling between *g* and *u* arises from terms in the kinetic energy describing the fact that the center of mass is no longer at the center of charge. At low nuclear velocities this coupling will be small.

More serious, and more common, are couplings with excited states of the same symmetry. These introduce coupling terms in the Schrödinger equation for the nuclear motion. Instead of simple phase shifts, the solution is then described[19] by a scattering matrix **S** that separates into two parts, $\mathbf{S}_u$ and $\mathbf{S}_g$. The coupling terms responsible for the transitions between states are electronic matrix elements depending on the internuclear distance *R*, and they can represent various types of interaction.

Besides a simple classification based on the magnitude of the interaction, we can classify them as to their dependence on the nuclear motion. Many of the electronic states interact with each other to a greater or lesser extent even if the nuclei are considered fixed. In addition, a coupling between the electronic and nuclear motion may permit a transition that would otherwise be forbidden, or may change the magnitude of a weak interaction. Such cases usually involve a coupling between the nuclear and electronic angular momenta that breaks a symmetry of the electronic state in a fixed nuclear frame.[20]

Coupling between states is most important where they approach in energy—or where they cross in some primitive approximation. The effect of the interaction in collisions often depends largely on the Landau-Zener parameter

$$w(R) = 2\pi H_{ij}^{el}(R)/\hbar v_R \left(\frac{d}{dR}\right) [H_{ii}^{el}(R) - H_{jj}^{el}(R)] \quad , \qquad (53)$$

where the electronic matrix elements H_{ij}^{el} are constructed by analogy with Eq. (3), and v_R is an average nuclear radial velocity near the crossing point R_x. If the nuclei are moving fast and $w(R)$ is small and close to the constant $w = w(R_x)$, the Landau-Zener result is obtained. In that case the probability of transition is small and equal to $(1 - e^{-w})$. The probability of transition is large when the nuclear velocity near R_x is small, *i.e.*, when the initial nuclear kinetic energy E is close to the energy $E_x + L^2/2\mu R_x^2$ of the crossing point. The simple Landau-Zener formula is then inapplicable, and we no longer have even a single nuclear velocity v_R; fortunately other treatments suitable for these conditions are now being investigated.[21] Qualitatively it is clear that for each transition $i \longleftrightarrow j$ there will be a characteristic range for the quantity

$$\epsilon = E - E_{x,ij} - L^2/2\mu(R_{x,ij})^2 \quad , \qquad (54)$$

in which transitions will have a high probability; this range will depend among other things on the magnitude of $H_{ij}^{el}(R_x)$. By setting $\epsilon = 0$ in Eq. (54) we get a relation between E and L such that the classical turning point coincides with the crossing point R_x; the domain of high transition probability lies in a band about this locus in the (E,L) plane. Since each (E,L) pair is associated primarily with an angle $\Theta_i(E,L)$ in the incoming state, the effect of the inelastic transition is to remove some

of the elastic flux from the angle $\theta = |\Theta_i(E,L)|$ and deposit it at a different energy, $E' = E - E_i^\infty + E_j^\infty$, and some new angle $\Theta_{ij}(E,L)$.

Curve crossings may be expected to have a further effect on the purely elastic scattering because the interaction may even alter the elastic phase $\Delta_i(E,L)$ when ϵ is small. This should happen especially when the crossing is of such a nature that the transition is to a bound state in an attractive well—a second crossing will leave the system back in the initial state on an outgoing course, but with a phase strikingly different from the phase associated with simple elastic scattering from the pure *incoming* potential. As a result we must expect some of the elastic flux to be shifted from its unperturbed position $|\Theta_i(E,L)|$, but to appear *elastically* at other angles where it will interfere coherently with the simple scattering.

In the case of interest here, the collision of ground state He and He^+, the prominent curve crossings with interaction involve g potentials only. Their effect on the final scattering appears therefore through $f_g(\theta)$. We have not attempted to calculate those effects here, but it is clear that they will make an important contribution to the damping of the oscillations as observed, just as they do in the case of $H^+ + H$.[8]

The major qualitative difference between the cases of He_2^+ and H_2^+ is that the helium ion shows curve crossings at finite (and even large) internuclear distances, while the hydrogen ion possesses no such crossings. Instead, in H_2^+ certain of the curves approach each other tangentially as $R \to 0$, the electronic energies of two different states each approaching the same united atom limit as R^2. The helium system also possesses tangential pseudocrossings of this type as $R \to 0$, since two or more curves may approach the same united atom level of Be^+, and the approach will generally occur quadratically as R. As Bates and others have pointed out, these tangential pseudocrossings are particularly efficacious in generating inelastic transitions because the interaction is strong over an extended region in R. Since they occur at small R, transitions of this kind are associated mainly with small L and large angles of scattering, at least at low energies.

Unlike H_2^+ then, He_2^+ possesses two types of pseudocrossings: linear ones at large R, and quadratic ones at $R = 0$. The latter type, which does exist in H_2^+, is likely to be especially important in He_2^+ as well. Both deserve to be studied.

III CALCULATIONS

A. POTENTIALS

The interaction potentials used in our calculations are illustrated in Fig. 1a. The attractive (ungerade) potential was obtained from the work of Reagen, Browne and Matsen[11], whose calculations cover the region from 0.8A to 5.0A. At $R = \infty$ this curve dissociates to $He(1s)^2$ and $He^+(1s)$. At $R = 0$ it is related to Be^+ in a $(1s)^2 2p$ configuration. Following the example of Lichten[7], the repulsive or gerade potential was obtained from the calculations of Phillipson[12] by use of Koopman's rule. These calculations cover the region from 0.5A to 2.0A. Phillipson's tables give the electronic energy which is related to the potential by Eq. (4). The value -130.58 eV was used for E_∞^{el}. For $R = 0$ this potential is related to a $Be^+(1s)(2p)^2$. Justification of the states to be used in the description of He^+ on He scattering has been given by Lichten[7]. Since the potentials were required for values of R down to 0.1A, the theoretical curves were extended to small values of R by assigning them a screened Coulomb form with arbitrary parameters. For large R they were allowed to decay exponentially.

Since derivatives of the potentials were also required, it was convenient to represent the potentials with analytical functions rather than use numerical values. The following functions fit the theoretical potentials within 1%.

$$V^u = \frac{80.6842}{R} \exp(-5.2529R) \qquad .5 < R$$

$$V^u = 2.300\{\exp[4.588(1-R/1.091)] - 2\exp[2.294(1-R/1.091)]\} \qquad .5 \leq R \leq 1.091$$

$$V^u = 2.300\{\exp[4.600(1-R/1.091)] - 2\exp[2.300(1-R/1.091)]\} \qquad 1.091 < R \leq 2.0$$

$$V^u = 2.698\{\exp[5.012(1-R/1.091)] - 2\exp[2.506(1-R/1.091)]\} \qquad 2.0 < R$$

$$V^g = \frac{73.0337}{R} \exp(-1.9018R) \qquad .7 < R$$

$$V^g = 7.75\exp[3.53(1-R/1.091)] \qquad .7 \leq R \leq 1.091$$

$$V^g = 7.75\exp[(3.2514(1-R/1.091)] \qquad 1.091 < R$$

Difficulties were encountered at junction points of these functions. Since the integrals involved in the calculations have singularities at R_0, any slight irregularities in the potential caused distortions in Θ_i when R_0 was near a junction point. These distortions were especially noticeable in the cross section curves near minima, since the minima are essentially small differences between large numbers. This difficulty was minimized by the use of smoothing routines in the offending regions.

The long range behavior of the potentials used in these calculations is not correct; however, for the range of energies and angles considered, it is irrelevant. The repulsive curve used in this work was always positive, while it is known that it must eventually become negative, *i.e.*, attractive. For H_2^+ the repulsive curve becomes attractive beyond 25A.[22] Since helium is less polarizable than hydrogen, the repulsive curve can only become attractive for $R > 25$A. The potentials used here also do not behave as R^{-4} at large R. Examination of the H_2^+ potentials and comparison of the work of Moiseiwitsch[23] and Dalgarno and Kingston[24] indicates that beyond 5A the polarization energy makes a significant contribution to the interaction potential. Undoubtedly at large R, the potentials used here are diminishing too rapidly. However, since we are dealing with relatively large incident energies (15 eV or greater) the long range forces essentially contribute only to very small scattering angles (less than 1°) and thus need not be considered. In fact, terminating the potential beyond 5.2A changed the phase shifts by less than one part in a thousand. On the other hand, changes in the g potential in the region between 2.0 and 5.0A had a considerable effect on the cross sections even though the turning point fell in the unaltered region, $R < 2.0$A.

The short range behavior (< 0.5A) of the potentials is also incorrect. A plot of V versus R looks reasonable at small R. However, if the coulombic repulsion term is subtracted from the potential and the resulting $E_{el}(R)$ is plotted as in Fig. 1b, it is readily apparent that the potentials do not have the proper small R behavior. Only the highest energy (300 eV) considered in this paper probes into this region of the potential, and that only at the larger angles. It would certainly be possible to guess at a better extrapolation of the potentials into this region, but what is really needed is an extension of the computed potentials to much smaller values of R.

B. CALCULATIONAL PROCEDURES

All calculations were performed on an IBM 7090. In general, integrals were evaluated by means of Gauss-Mehler[25] quadratures. The machine programs were checked by hand calculations and by using a 6-12 potential and comparing with tabulated values.[26] Values obtained by Gauss-Mehler quadratures were also verified by evaluating the integrals by Weddle's Rule.[27]

The quantities necessary for the calculation of the classical scattering amplitudes whose interference gives the differential cross section in the semiclassical approximation are the phases, Δ_i, the deflection functions, Θ_i, and the derivative of Θ_i with respect to L, Γ_i. The phase is given by Eq. (25a). The other quantities are given by

$$\Theta = \frac{\partial \Delta}{\partial L} = \Pi - 2L \int_{R_0}^{\infty} \frac{dR}{R^2 \left[2\mu [E - V(R)] - \frac{L^2}{R^2} \right]^{1/2}} \tag{55}$$

$$\Gamma = \frac{\partial^2 \Delta}{\partial L^2} = A \cdot \int_{R_0}^{\infty} \frac{R \left[\frac{V'(R)}{V'(R_0)} - \frac{E - V(R)}{E - V(R_0)} \right] dR}{\left[\frac{E - V(R)}{E - V(R_0)} \cdot R^2 - R_0^2 \right]^{3/2}} \tag{56}$$

where the prime denotes differentiation with respect to R and

$$A = -\frac{1}{L} \frac{2R_0^2 V'(R_0)}{\left[\frac{L^2}{\mu R_0^2} - R_0 V'(R_0) \right]} \tag{56a}$$

The calculational program used was the following. Δ, Θ and Γ were evaluated for various values of L at each energy E. An adequate variation

in L was used so that the desired range in Θ was covered. Sufficient values were computed to permit accurate interpolation of L, Δ, and Γ at successive values of Θ. The cross sections were then evaluated by means of Eqs. (26), (21) and (40).

To test the validity of the semiclassical approximation a program was developed to calculate the cross sections by the semiquantal summation procedure. Converting the classical phase, $\Delta(L)$, into a quantum phase shift δ_l by means of Eq. (24) we obtain an expression for δ_l which is a valid approximation in this case since the reduced energy (E/ϵ) is greater than 5 and the quantum parameter, Λ^+, is less than 0.2[28]. For small and moderate ℓ values the phase shifts were evaluated by Weddle's Rule. For large ℓ (more precisely, large R_0) the expression for the phase shift reduces to

$$\delta_l = -\frac{\mu}{\hbar^2 k}\int_{R_0}^{\infty}\frac{V(r)dR}{[1-\beta^2/R^2]^{1/2}} \tag{57}$$

and to an excellent approximation

$$\beta \equiv \frac{(l+1/2)}{k} \approx R_0$$

Since the potentials were written in an exponential form, the phase shifts are given by

$$\delta_l = \frac{\mu \cdot c}{\hbar^2 k}\int_{R_0}^{\infty}\frac{Re^{-\gamma R}}{[R^2-R_0^2]^{1/2}}dR \tag{58}$$

where c and γ are potential parameters. This integral may be evaluated to yield[29]

$$\delta_l = \frac{\mu \cdot c}{\hbar^2 k}\cdot R_0 \cdot K_1(\gamma R_0) \tag{59}$$

where K_1 is the first order modified Bessel function of the second kind. For large values of γR_0, which is the case here, K_1 may be expanded as a rapidly converging series.[30] For E = 15 eV and the He^+ - He system the above equation was valid for $l > 325$ (criterion: the difference between the semiclassical phase shift and Eq. (59) is less than .005 radians). 500 phase shifts were found to be sufficient for the cross section to be accurate to at least 3 significant figures. The cross sections were evaluated by means of Eqs. (23), (21) and (40).

The reliability of the semiclassical calculation is shown at 15 eV by its comparison with the semiquantal one in Fig. 2. Outside the rainbow angle the only noticeable discrepancy is in the absolute magnitude of the fine structure. On the low angle side of the rainbow region greater deviations appear; they are due to known deficiencies of the rainbow approximation. Neither of these features is of any significance in the comparison of theory with experiment because they appear only at much finer angular resolution than the experiments allow. For that reason, we used only the semiclassical method at higher energies, where it should be still more reliable.

Calculations were also performed in the vicinity of the rainbow angle using a modified semiclassical approximation. In this region $\Theta_u(L)$ may be expanded as a quadratic about the classical rainbow angle, θ_r^{cl}. The resulting expressions contain Airy integrals for which extensive tables[31] are available. A lucid discussion and the relevant equations for this procedure have been given by Ford and Wheeler.[16] On the dark (large angle) side of the rainbow angle this approximation blends in smoothly with the usual semiclassical approximation. On the bright side, however, it does not, since a quadratic expansion of the deflection function is a poor representation for Θ_u at large L (small angles). For this reason Fig. 2 shows the semiclassical approximation only for angles greater than 6°. The rainbow angle cross sections were computed ignoring the effect of nuclear symmetry; Fig. 4 shows that this effect is negligible at small angles.

IV RESULTS AND DISCUSSION

A. ELASTIC EFFECTS

Figures 2, 3, and 4 show our calculated differential scattering cross sections at 15, 50 and 300 eV and the corresponding experimental results. We have used center mass energies and angles throughout, which means that our energies are half the laboratory energies and angles twice the laboratory angles.

Two features of our calculations provide qualitatively new explanations for phenomena seen in the experimental data. First, the correct treatment of the interference between gerade and ungerade scattering (as also observed by F. J. Smith[10]) gives a second mechanism for the "damping" of the interference oscillations which may, at low energies, be more important than the effect of inelastic processes. Second, the additional interference due to nuclear symmetry explains the subsidiary structure seen on the main interference peaks in the experiments at large angles, especially at energies above 100 eV.

The effect of nuclear symmetry is shown in the curve at 300 eV, Fig. 4, where the full theoretical curve is compared with the contributions from direct scattering and pure charge exchange scattering. Out to about 20° the full curve coincides well with the pure direct scattering contribution. The pure exchange contribution is insignificant out to at least 40°, but the interference between the two has an intermediate magnitude and becomes important in the region from 20° out. An analysis of the phases following Eqs. (46) to (49) shows that this subsidiary structure oscillates about 3 times faster than the main peaks near 25° and about 6-7 times faster near 50°. This behavior is shown in Fig. 4, and just these periods can be seen in the fine structure of the experimental curve. Similar structure can be identified with varying degrees of resolution in all the experimental curves except those at the lowest energies (10 and 15 eV)[1], where the resolution is insufficient.

We believe that the identification of the experimental fine structure as an effect of nuclear symmetry is firmly grounded in the identity of the theoretical and experimental periodicities. Further tests can be made to

confirm this conclusion. First, we can predict the direction and rate of movement of the peaks with energy. Second, this interference effect should not appear in the unsymmetric scattering events $^4He^+ + {}^3He$ and $^3He^+ + {}^4He$.

The movement of the subsidiary peaks with energy can be examined experimentally with the aid of a plot of the loci of the maxima and minima in the (E,θ) plane, as employed by Everhart[2c]. Such a diagram is given for the main peaks by Lorents and Aberth[1], and a similar one could be constructed for the subsidiary peaks. A theoretical prediction of the movement of these features can be made by using Eqs. (52) combined with (47) to (49); note that the first term in Eq. (49) suggests that maxima tend to turn into minima when the sign of $\cos \epsilon_{12}$ changes. A preliminary estimate suggests that at energies near 300 eV and in the angular region 20° to 60° the secondary peaks will move in the opposite direction to the main peaks and up to 5 times faster. In order to follow this motion and identify the peaks properly, experiments may be needed at energies considerably closer than the 50 eV intervals thus far measured.

In a quantitative comparison between theory and experiment, the sources of disagreement are of three main types. First, the experimental limitations on resolution and sensitivity discussed in Ref. 1, especially: (a) the geometric limitation on angular resolution (slit sizes, shapes and locations), (b) the effect of the thermal motion of the target atoms on angular resolution, and (c) the background noise limit on sensitivity. Second, the intrinsic limitations of a 2-state theory, which does not take into account inelastic collisions or the effect of other molecular states on the elastic collision. Third, inaccuracy of the potential functions used in our 2-state calculations. These factors of disagreement work in varying ways on the different features of the curves that are available for the comparison of theory and experiment.

The principal features of the curves that can be examined are (1) the principal maxima and minima, especially (a) their periodicity, (b) their movement with energy, and (c) their precise location; (2) the subsidiary extrema, in the same ways; (3) the rainbow scattering region, (a) its location and (b) its general behavior; and (4) the absolute magnitude of the cross section curve, with regard to which we may consider several degrees of resolution, (a) the upper envelope, (b) the lower envelope of the principal peaks, (c) the amplitudes of the secondary peaks, and (d) the curve in complete detail. We see immediately from the figures that the

principal peaks are well explained in their periodicity and their movement with energy, but their location is less precisely given, especially at low energy and at the largest angles. The periodicity of the subsidiary peaks seems will accounted for, but their movement has not yet been explored experimentally, and their exact locations cannot be predicted as yet because they depend sensitively on the potential in the small R region where it is not really known and where our extrapolations fail. The rainbow angle is in complete agreement with prediction, confirming the ungerade potential near its minimum; the detailed rainbow behavior is masked by lack of angular resolution, but its average behavior is satisfactory, as shown by Fig. ( ) of Ref. (1) where the experimental angular distribution is taken into account. The magnitudes of the cross section curves show quite satisfactory agreement, the upper envelopes matching well within experimental error except in the large angle region ($\theta \gtrsim 40°$ at 50 eV and $\theta \gtrsim 20°$ at 300 eV) where the calculations reflect inaccuracies in the potential. The calculated lower envelope lies consistently below the experimental one, an expected result of limited angular resolution and background noise. The amplitudes of even the secondary oscillations show considerable agreement with experiment (perhaps fortuitously) at 300 eV, but at 50 eV they seem too large; with improved potentials the secondary peaks may change considerably.

It has been our aim here to show how well the existing potentials explain the experimental results. However, the data are of such quality that they can also be used to improve our knowledge of the potentials, and we intend to pursue this inverse problem later. This seems especially worth while because the 3-electron diatomic system He_2^+ is an ideal test case for comparing theory and experiment. We hope that the experiments and our calculations will prompt further work on the electronic states of this system. Better estimates of the potentials are needed, especially for $R \leq 0.8$A for the u curve and for $R \leq 0.5$A as well as $2.0\text{A} < R < 5.0\text{A}$ for the g. An examination of the classical turning points shows that the experiments at large angles probe into regions of small R where the potentials are ill known; this is especially important in that the integrals involved in computing $f(\theta)$ weight the region of the classical turning point strongly. Conversely, this makes it possible to see what region of the potential should be adjusted in order to fit the data better.

In connection with the inverse problem, it is worth noting that the sum of the upper and lower envelopes of the cross section curve depends

mainly on the average potential, by Eqs. (38a and b):

$$\sigma(E,\theta) \cong \sigma_+ + \sigma_- \quad .$$

The lower envelope

$$\sigma_- \cong \frac{\delta\sigma^2}{4\sigma}$$

gives us a function $\delta\sigma$ that depends on the difference potential as well as the average. The difference potential appears also in the phase difference $\delta A(E,\theta) = (A_g - A_u)_\theta$ which is responsible for the location of the maxima and minima of the inteference pattern. Since $\delta A(E,\theta)$ is given very well experimentally, the difference potential can be deduced by inverting Eq. (37). A computation of the lower envelope σ_- can then be used as a check on the potentials deduced in this way.

B. INELASTIC EFFECTS

Inelastic collisions probably do not affect the elastic cross section curves much at these low energies. The ungerade state in particular can hardly participate at all in inelastic events at these energies since no other states of the same symmetry approach it—a similar case is seen in the collision $H^+ + He$, where the ground state collision involves an isolated curve and the inelastic charge exchange process exceeds 5% of the total only at energies above 5 keV where nuclear and electronic velocities begin to be comparable.[32] Inelastic processes can occur in the gerade state, where there are many curve crossings, but each inelastic transition probably is confined to a rather narrow band in (E,L) space, in which case its chief effect on the elastic cross section is to make $f_g(E,\theta)$ somewhat smaller in a certain range of θ. Without inelastic transitions we have $|f_g(E,\theta)| > |f_u(E,\theta)|$ for all θ larger than the rainbow angle at the energies we have investigated. Since the envelopes are the upper and lower limits of the inequality

$$\big|\,|f_g| - |f_u|\,\big| \le |f_g + f_u| \le |f_g| + |f_u|,$$

a decrease in $|f_g|$ will lower the maxima, but it will lower the minima still more. This shows strikingly that the first effect of inelastic transitions among g states is to *decrease* the damping of the oscillations predicted in Figs. 2-4. Only if inelastic effects become so pronounced

as to make $|f_g|<|f_u|$ will they begin to dominate over the 2-state interference effect in the damping—the smaller $|f_g|-|f_u|$ in the 2-state theory, the sooner this will occur.

Inelastic effects can never contribute to the interferences seen in the elastic cross section except by reducing the magnitude of some $f_i(\theta)$. However, a related elastic effect may also arise from the curve crossings that produce the low energy inelastic transitions: In the neighborhood of a curve crossing the phase of the elastic partial waves may be altered by the interaction, producing an anomalous contribution to $f(\theta)$. If, as is likely, this spreads its effect widely in θ, its magnitude will be small everywhere and it will only be noticeable (if at all) by its diminution of the unperturbed $f_i(\theta)$ near the crossing angle. However, a strong interaction of 2 or more electronic states may result in a shift of the phase of one of the elastic f_i's which will then show itself in the elastic interference pattern. Such an effect was detected by Bates and Williams[8] in the case of $H^+ + H$ at relatively high energies due to the tangential pseudocrossing of 2 states at small R. In $He^+ + He$ such effects are probably confined to still higher energies, because of the greater coulomb repulsion.

A quantitative discussion of inelastic scattering and of the elastic effect of curve crossings and approaches can only be carried out in the framework of a general theory of curve crossing. Fortunately, that theory is undergoing rapid development now.[21,33] Its application to this problem, including the inelastic cross sections now being observed by Lorents and Aberth[1], must be left to later work.

C. CONCLUSIONS

A 2-state theory, using the diabatic potential curves advocated by Lichten,[7] appears adequate to describe quantitatively all the major features seen experimentally in the elastic scattering of He^+ on He in the energy range up to 300 eV, including the non-zero minima of the interference pattern and the secondary oscillations. These secondary oscillations are probably due to nuclear symmetry, and an experiment has been proposed to confirm this by scattering $^4He^+$ on ^3He. In the region in which they have been carefully computed, the u potential of Reagan, Browne and Matsen[11] and the g potential of Phillipson[12] and Lichten[7] are satisfactory, but the experiments at large angle and energy probe to

regions of small R, and the experiments at low energy depend on regions of large R, where the potentials have not been adequately computed as yet. We advocate extension of the potential calculations into those regions.

The system studied here, $He^+ + He$, is one of a relatively small number of diatomic combinations that can be thoroughly studied at present both experimentally and theoretically. The agreement between theory and experiment in the elastic scattering is a gratifying test of the adequacy of our theoretical understanding and of the approximations used in the computations. It is even more important to extend this test to the inelastic collisions that are a greater theoretical challenge. An extension of the elastic calculations into the regions where the potentials are presently defective is an essential prelude to a thorough study of the inelastic scattering.

The symmetry of the coulomb field in He_2^+ allows strict separation of the wave functions into two parts, one g and one u. A 2-state theory of this collision is really just a superposition of two 1-state solutions, and in that sense the theory we have been using is a very restricted 2-state theory. The real problems of a 2-state theory come in when it deals with states that do interact with each other, as they must in any theory of inelastic processes. Such interactions can influence even the elastic scattering (by the interactions of two or more g states, for example). The possibility of detecting such a perturbation in the elastic scattering is one of the reasons for pursuing further the theoretical and experimental study of the elastic collisions as well as the inelastic ones.

ACKNOWLEDGMENT

The authors wish to thank Drs. Lorents and Aberth of Stanford Research Institute and Dr. B. Moiseiwitsch of the Queen's University of Belfast for many helpful discussions.

REFERENCES

* This work principally supported by the National Aeronautics and Space Administration and in part by the National Science Foundation.

1. D. C. Lorents and W. Aberth, preceding paper.

2. (a) F. P. Ziemba and E. Everhart, Phys. Rev. Letters, **2**, 299 (1959).
(b) G. J. Lockwood, H. F. Helbig and E. Everhart, Phys. Rev., **132**, 2078 (1963).
(c) E. Everhart, Phys. Rev., **132**, 2083 (1963).

3. M. F. Mott, Proc. Roy. Soc. (A), **126**, 259 (1930).

4. H. S. W. Massey and R. A. Smith, Proc. Roy. Soc. (A), **142**, 142 (1933).

5. L. Pauling, J. Chem. Phys., **1**, 56 (1933).

6. F. P. Ziemba and A. Russek, Phys. Rev., **115**, 922 (1959).

7. W. L. Lichten, Phys. Rev., **131**, 229 (1963).

8. D. R. Bates and D. A. Williams, Proc. Phys. Soc., **83**, 425 (1964).

9. F. T. Smith, Bull. Am. Phys. Soc., **9**, 411 (1964).

10. F. J. Smith, Phys. Letters (Netherlands), **10**, 290 (1964).

11. P. N. Reagan, J. C. Browne and F. A. Matsen, Phys. Rev., **132**, 304 (1963).

12. P. E. Phillipson, Phys. Rev., **125**, 1981 (1962).

13. E. C. G. Stueckelberg, Helv. Phys. Acta, **5**, 370 (1932).

14. D. R. Bates and A. H. Boyd, Proc. Phys. Soc., **80**, 1301 (1962).

15. F. T. Smith, "Classical and Quantal Scattering. I. The Classical Action," J. Chem. Phys., to be published.

16. N. F. Mott and H. S. W. Massey, *The Theory of Atom Collisions* (Clarendon Press, Oxford, 1933).

17. K. W. Ford and J. A. Wheeler, Ann. Phys., **7**, 259 (1959).

18. Cf. T. Y. Wu and T. Ohmura, *Quantum Theory of Scattering*, pp. 235-237 (Prentice-Hall Inc., Englewood Cliffs, N.J., 1962). Also, J. O. Hirschfelder, C. F. Curtiss and R. B. Bird, *Molecular Theory of Gases and Liquids*, p. 74 (John Wiley and Sons, Inc., New York, 1954).

19. D. R. Bates, H. S. W. Massey and A. L. Stewart, Proc. Roy. Soc. (A), **216**, 437 (1953).

20. W. R. Thorson, J. Chem. Phys., **39**, 1431 (1963); W. R. Thorson, p. 964 in *Atomic Collision Processes* (M. C. R. McDowell, ed., North Holland Publishing Co., Amsterdam, 1964); and W. R. Thorson and A. D. Bandrank, J. Chem. Phys., **41**, 2503 (1964).

21. See, for instance, V. K. Bykhovsky, E. E. Nikitin, and M. Ya. Ovchinnikova, J. Exptl. Theoret. Phys. (USSR) **47**, 750 (1964), as an example of much recent Russian work. Bates and the Belfast group are also active in this problem [*e.g.*, Ref. (8)].

22. A. Dalgarno and J. T. Lewis, Proc. Phys. Soc., **A67**, 57 (1956).

23. B. L. Moiseiwitsch, Proc. Phys. Soc., **A69**, 653 (1956).

24. A. Dalgarno and A. E. Kingston, Proc. Phys. Soc., **73**, 455 (1959).

25. F. J. Smith, Physica, **30**, 497 (1964); Z. Kopal, "Numerical Analysis" (John Wiley and Sons, Inc., N.Y., 1961).

26. R. B. Bernstein, J. Chem. Phys., **33**, 795 (1960).

27. J. B. Scarborough, *Numerical Mathematical Analysis* (John Hopkins Press, Baltimore, 1955), 3rd Ed.

28. R. J. Munn, E. A. Mason and F. J. Smith, "Some Aspects of the Quantal and Semiclassical Calculations of Phase Shifts and Cross Sections for Molecular Scattering and Transport," Institute of Molecular Physics, University of Maryland. IMP-NASA-38, July 31, 1964.

29. *Tables of Integral Transforms*, Bateman Manuscript Project, Vol. I, p. 136 (McGraw-Hill Book Co., Inc., New York, Toronto, London, 1954).

30. E. T. Whittaker and G. N. Watson, *Modern Analysis*, p. 374 (The Macmillan Co., New York, 1947).

31. J. C. P. Miller, *The Airy Integral* (British Association for Advancement of Science, Math. Tables, Part-Volume B. Cambridge Univ. Press, London and New York, 1946).

32. H. F. Helbig and E. Everhart, Phys. Rev. **136**, A674 (1964).

Figure Captions

Figure 1a: Theoretical gerade and ungerade potentials.

Figure 1b: Gerade and ungerade electronic energies used in this paper. Dashed lines indicate a more realistic behavior.

Figure 2: Comparison of differential cross sections (center of mass coordinate system) at 15 eV. The insert compares the two theoretical methods of calculation in the vicinity of the rainbow angle.

Figure 3: Theoretical and experimental differential cross sections versus scattering angle at 50 eV.

Figure 4: Comparison of differential cross sections at 300 eV. The — — — curve is σ_{AA} of Eq. (21) and the — . — curve is σ_{AB} of Eq. (21) but evaluated at $\pi - \theta$. The solid curve is the sum of $\sigma_{AA}(\theta)$ and $\sigma_{AB}(\pi - \theta)$ plus cross terms [see Eq. (40)].

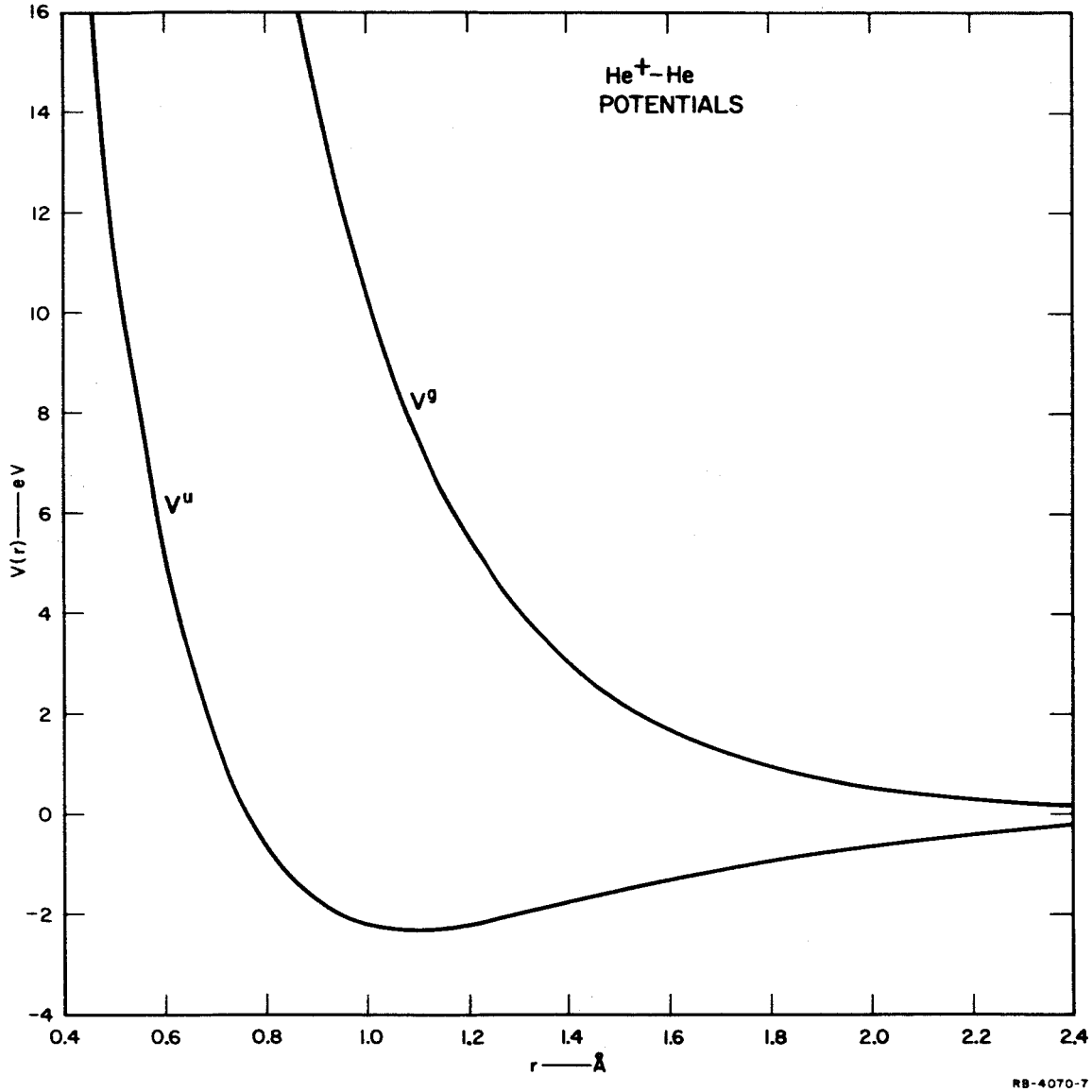
He+-He
POTENTIALS
V^g
V^u
V(r)——eV
r——Å
16
14
12
10
8
6
4
2
0
-2
-4
0.4
0.6
0.8
1.0
1.2
1.4
1.6
1.8
2.0
2.2
2.4
RB-4070-7

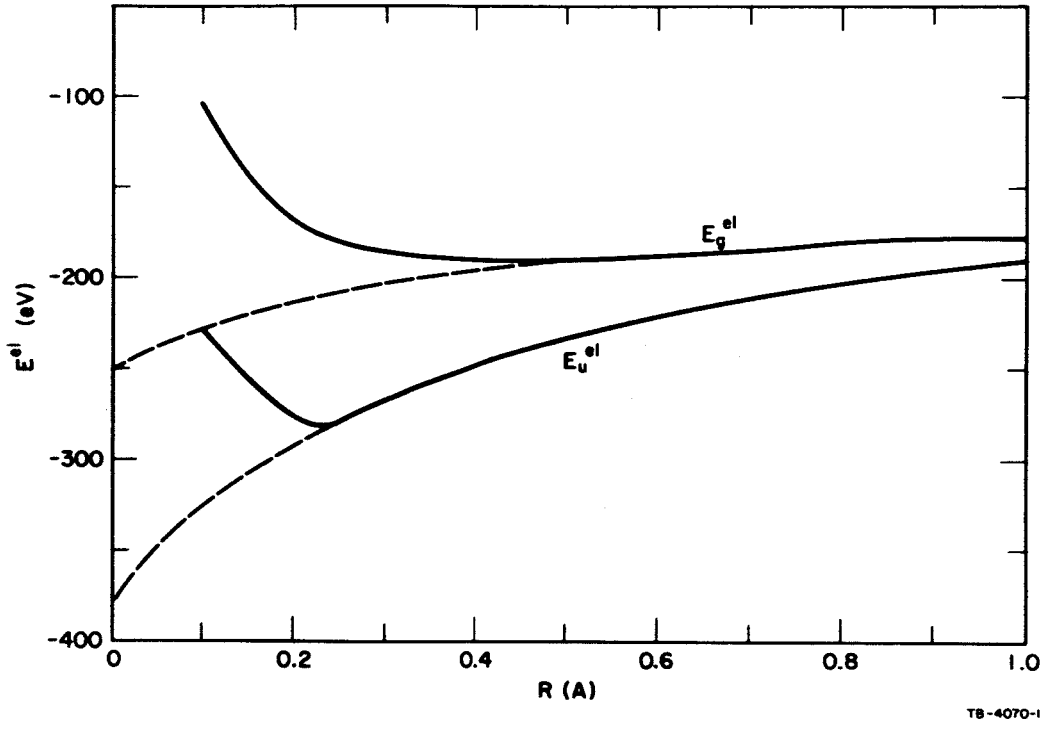
-100
-200
-300
-400
E^{el} (eV)
E_g^{el}
E_u^{el}
0
0.2
0.4
0.6
0.8
1.0
R (A)
TB-4070-1

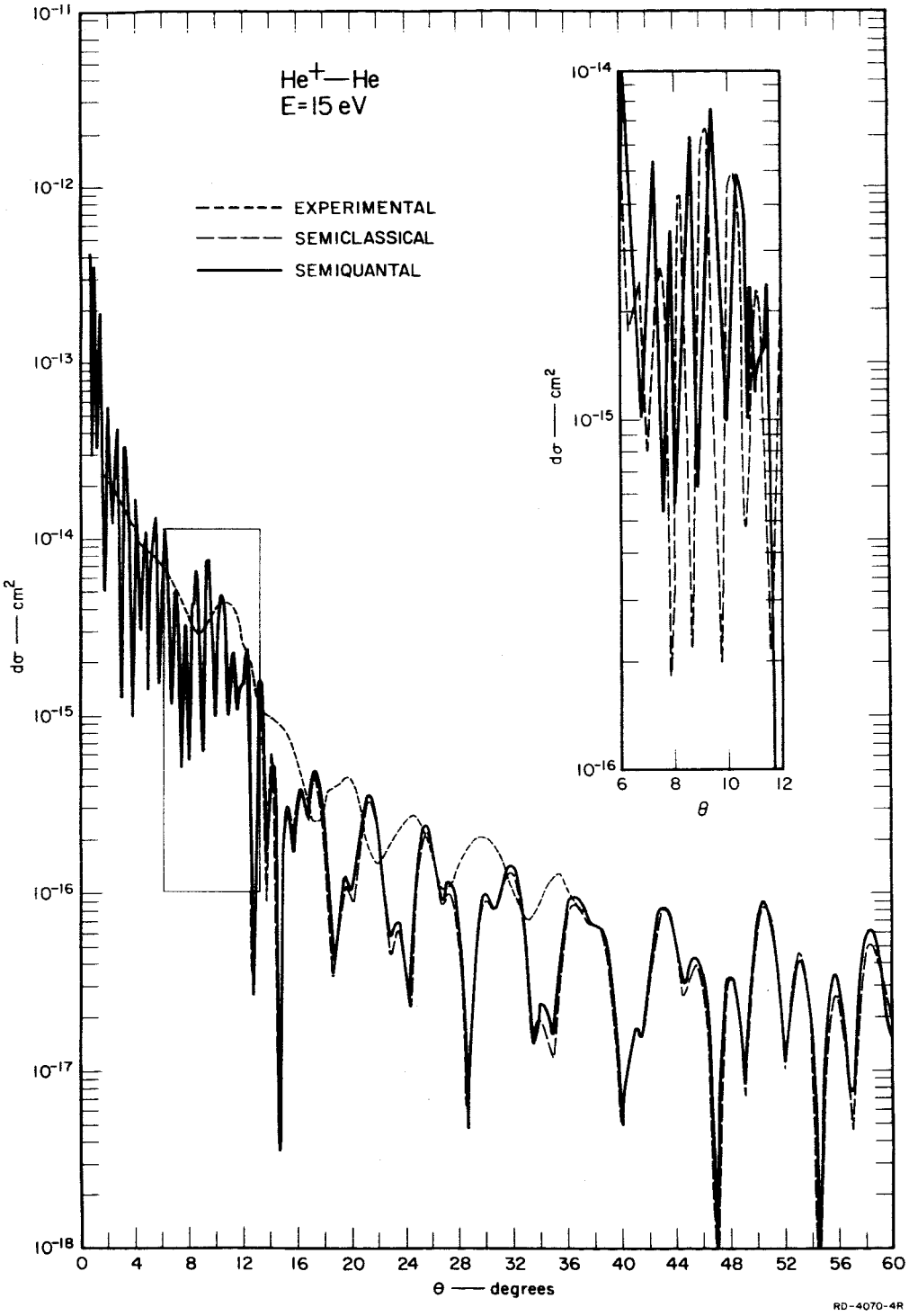
He+—He
E=15 eV
EXPERIMENTAL
SEMICLASSICAL
SEMIQUANTAL
dσ — cm²
θ — degrees
θ
RD-4070-4R

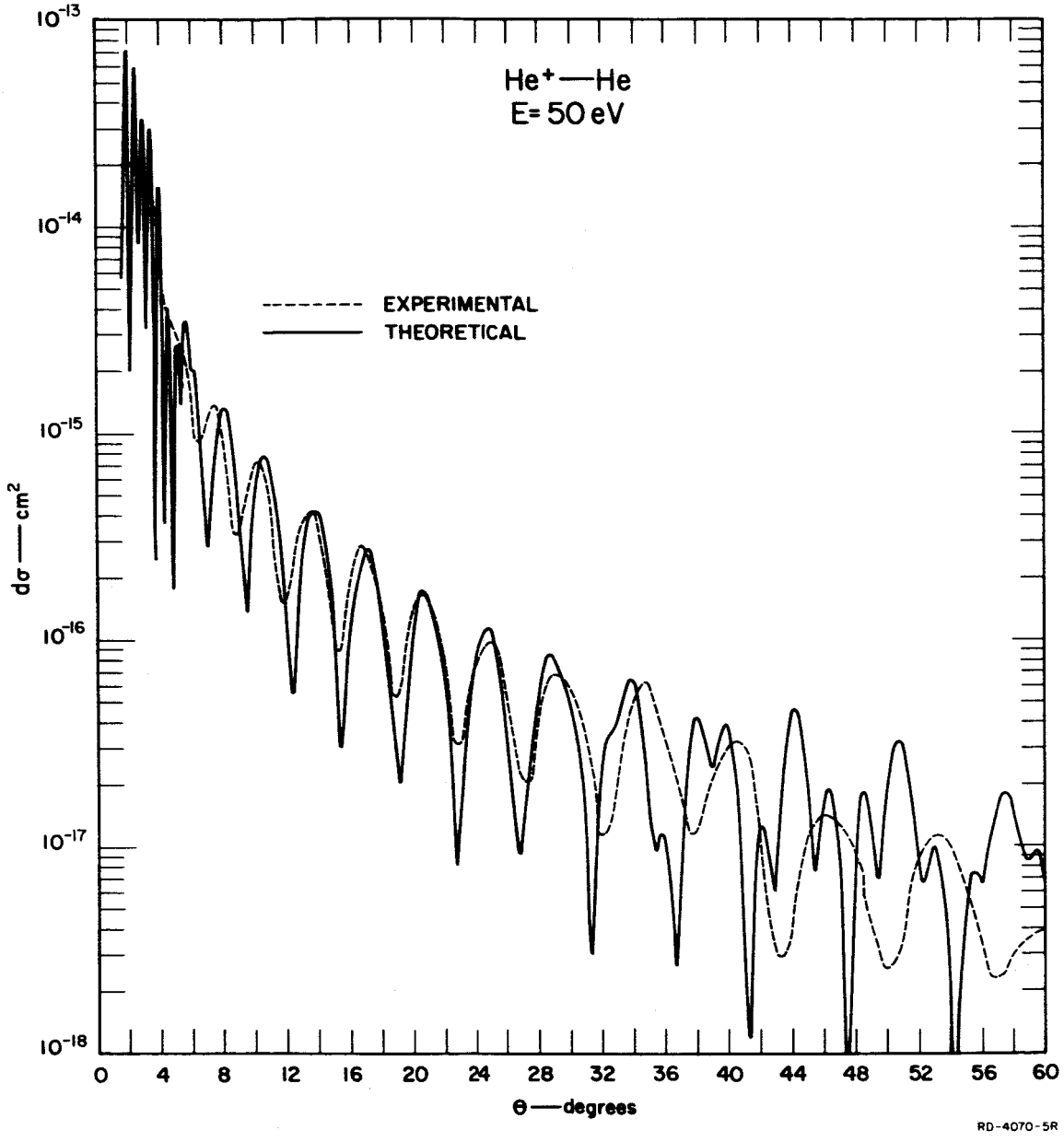
He+—He
E= 50 eV
EXPERIMENTAL
THEORETICAL
dσ — cm²
10⁻¹³
10⁻¹⁴
10⁻¹⁵
10⁻¹⁶
10⁻¹⁷
10⁻¹⁸
0
4
8
12
16
20
24
28
32
36
40
44
48
52
56
60
θ — degrees
RD-4070-5R

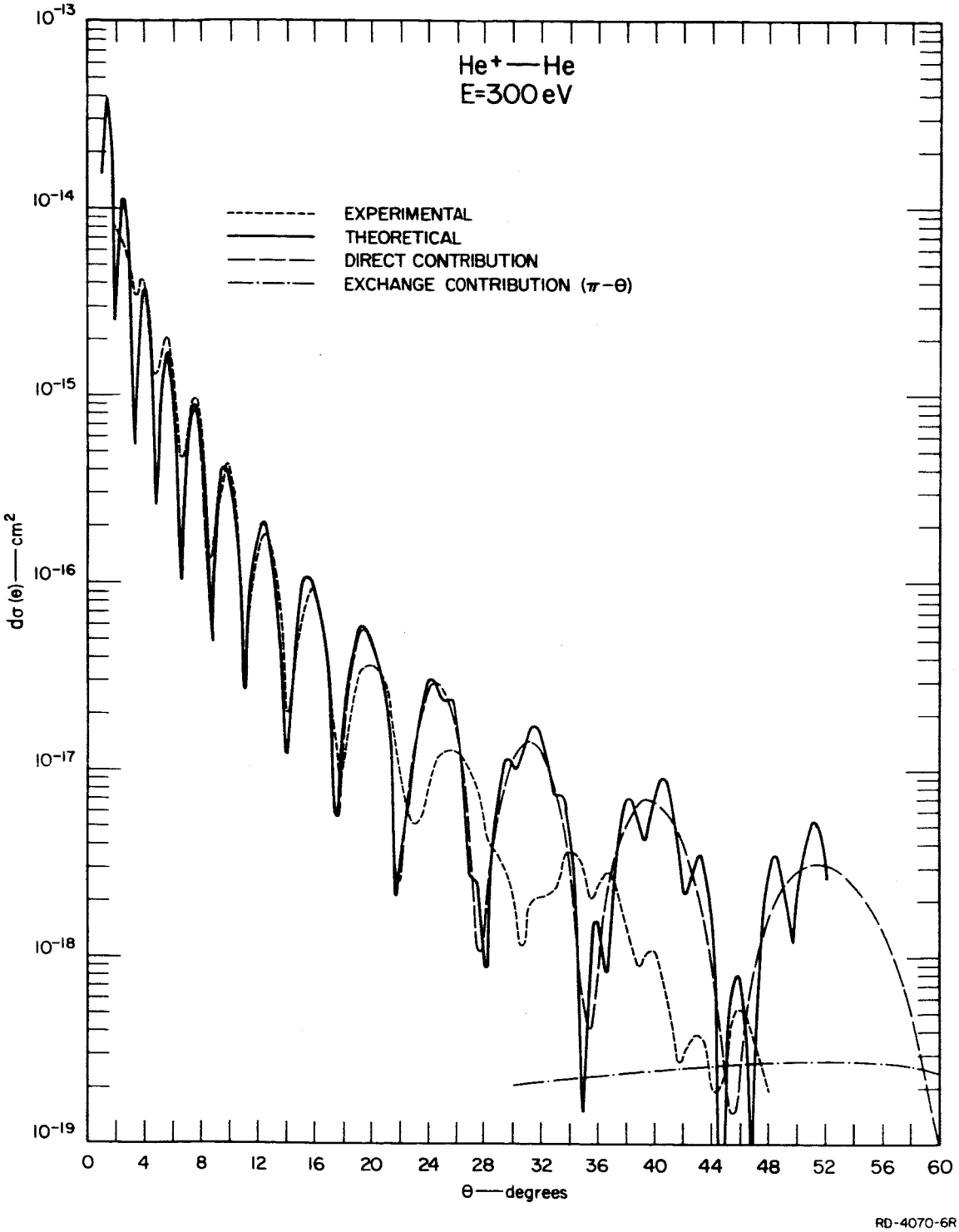
He+—He
E=300 eV
EXPERIMENTAL
THEORETICAL
DIRECT CONTRIBUTION
EXCHANGE CONTRIBUTION (π−θ)
dσ(θ)—cm²
θ—degrees
RD-4070-6R